

Dalton Transactions

Accepted Manuscript



This is an *Accepted Manuscript*, which has been through the Royal Society of Chemistry peer review process and has been accepted for publication.

Accepted Manuscripts are published online shortly after acceptance, before technical editing, formatting and proof reading. Using this free service, authors can make their results available to the community, in citable form, before we publish the edited article. We will replace this *Accepted Manuscript* with the edited and formatted *Advance Article* as soon as it is available.

You can find more information about *Accepted Manuscripts* in the [Information for Authors](#).

Please note that technical editing may introduce minor changes to the text and/or graphics, which may alter content. The journal's standard [Terms & Conditions](#) and the [Ethical guidelines](#) still apply. In no event shall the Royal Society of Chemistry be held responsible for any errors or omissions in this *Accepted Manuscript* or any consequences arising from the use of any information it contains.



ARTICLE

Ni²⁺-zeolite/ferrosphere and Ni²⁺-silica/ferrosphere beads for magnetic affinity separation of histidine-tagged proteins

T. A. Vereshchagina,^a M. A. Fedorchak,^a O. M. Sharonova,^a E. V. Fomenko,^a N. N. Shishkina,^a A. M. Zhizhaev,^a A. N. Kudryavtsev,^b L. A. Frank^{b,c} and A. G. Anshits^{a,c}

Received 00th January 20xx,
Accepted 00th January 20xx

DOI: 10.1039/x0xx00000x

www.rsc.org/

Magnetic Ni²⁺-zeolite/ferrosphere and Ni²⁺-silica/ferrosphere beads (Ni-Ferrosphere Beads - NFB) of a core-shell structure were synthesized starting from coal fly ash ferrospheres having diameters in the range of 0.063-0.050 mm. The strategy of NFB fabrication is an oriented chemical modification of outer surface preserving the magnetic core of parent beads with formation of microporous coverings. Two routes of ferrosphere modification were realized, such as (i) hydrothermal treatment in an alkaline medium resulting in a NaP zeolite layer and (ii) synthesis of microporous silica on the glass surface using conventional methods. Immobilization of Ni²⁺ ions in the siliceous porous shell of the magnetic beads was carried out via (i) the ion exchange of Na⁺ for Ni²⁺ in the zeolite layer or (ii) deposition of NiO clusters in the zeolite and silica pores. The final NFB were tested for affinity in magnetic separation of the histidine-tagged green fluorescent protein (GFP) directly from a cell lysate. Results pointed to the high affinity of the magnetic beads towards the protein in the presence of 10 mM EDTA. The sorption capacity of the ferrosphere based Ni-beads with respect to GFP was in the range 1.5-5.7 mg·cm⁻³.

Introduction

Methods of expression and selective isolation of target proteins and peptides from biological liquids, e.g. cell lysates and sera, play an important part in proteomics and biomedical research, especially, in molecular diagnostics of socially-significant diseases.¹⁻³ Immobilized-metal affinity chromatography (IMAC) is among the most promising methods for separation of recombinant proteins tagged with a sequence of six or more histidine residues (His-tag) which are bound to the N or C terminal of the recombinant protein and exhibits a high affinity towards metal ions such as nickel (Ni²⁺), zinc (Zn²⁺), cobalt (Co²⁺), copper (Cu²⁺), etc.³⁻⁶ Metal ions are usually immobilized to a solid support by means of coordination bonds with the tri-, tetra- or pentadentate chelating ligand attached to the surface. Free valencies of the chelated metal ion are used to capture a target protein by interacting with electron donating nitrogen atoms of the histidine tag. The trapped protein can be easily released by elution with the stronger chelating agent, such as imidazole or EDTA. Nickel-nitrilotriacetic acid (Ni-NTA) beads are most popularly used to purify His-tag proteins.³

Despite the wide compatibility, IMAC based on metal ion chelated sorbents has some limitations.³ First of all, the use of complexing agents (EDTA, imidazole, and histidine) in the protein expression system has to be avoided. Secondly, recharge of the sorbent is required after the elution step because of its deactivation due to washing-out metal ions by imidazole.⁷ And, finally, long operation time in a dynamic mode restricts application of the IMAC technique on a large scale, for example, in industrial-scale production of biopharmaceuticals.

To solve these problems, some modifications in preparation procedures of IMAC sorbents have been suggested, such as (i) immobilization of metal ions on solid supports by ionic⁸ or covalent binding without use of any chelating ligand⁹⁻¹² and/or (ii) the use of magnetic supports for fixing metal ions to facilitate the protein separation applying a magnetic field.¹⁰⁻²⁰ Only a few magnetic separation systems based on metal ion chelated particles are commercially available, such as Ni-NTA magnetic agarose beads (Qiagen, Germany)¹⁷, Talon® magnetic resin charged with Co²⁺ by complexation with tetradentate carboxymethyl aspartate (Clontech, USA)¹⁸, silica-based SiMAG-IDA/Nickel particles (Chemicell, Germany), and BcMag™ His-Ni Magnetic Beads (BioClone, Canada) fabricated with the use of iminodiacetic acid (IDA).^{19,20} The binding capacity of the commercial affine sorbents regarding proteins of an average size (20-30 kDa) is in the range of 1-15 mg·cm⁻³ beads.

Combination of magnetic properties with strong immobilization of metal ions in a sorbent shell seems to be

^a Institute of Chemistry and Chemical Technology SB RAS, 50/24 Akademgorodok, Krasnoyarsk, 660036, Russia. Fax: +7 391 249 4108; Tel: +7 391 205 1944; E-mail: tatiana_ver@mail.ru.

^b Institute of Biophysics SB RAS, 50/50 Akademgorodok, Krasnoyarsk, 660036, Russia. Fax: +7 391 2433400; Tel: +7 391 249 4430; E-mail: lfrank@yandex.ru

^c Siberian Federal University, 79 Svobodnyi Avenue, Krasnoyarsk, 660041, Russia. Fax: +7 391 2912108; Tel: +7 391 249 7559; E-mail: anshits@icct.ru.

optimal to overcome limitations mentioned above. A number of nano- and microsized magnetic core-shell systems of this type have been reported, such as Ni²⁺-silica coated magnetite beads (Ni²⁺-SiMAG, Chemcell),¹⁰ Zn²⁺-decorated maghemite/silica particles,¹¹ yolk-shell nanostructured Fe₃O₄/NiSiO₃ beads.¹² In contrast to the magnetic Ni-NTA agarose beads and similar sorbents, a magnetic core of all the systems is covered by a metal ion/silica matrix with the metal ions tightly integrated in the silica by covalent binding. With the SiMAG beads, this approach results in improved purification of histidine-tagged proteins from crude bacterial extracts and repeated recycling without reactivation of the sorbent.¹⁰ Kim et al.¹³ have designed a magnetically recyclable nanocomposite microspheres for protein separation by combining ferromagnetic magnetite cores and NiO nanoparticles incorporated onto a mesoporous silica shell. Authors concluded that this novel separation system might overcome the problem of the low magnetic moment of magnetic separation systems fabricated with use of magnetic nanoparticles.

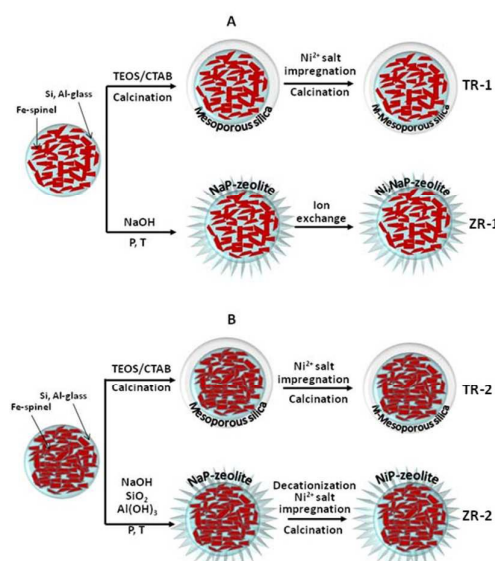
The majority of methods to synthesize magnetic composites with a magnetic core based on iron oxides are time-consuming multi-step procedures, certain of it being realized under reductive conditions (for example, H₂/N₂).¹³ The synthesis of magnetic sorbents can be substantially simplified using ready-made magnetic beads, such as fly ash ferrospheres (Fs).²¹⁻²³ Ferrospheres are resulted from combustion of pulverized coal at heat power plants in the process of thermochemical conversion of iron-bearing mineral matter of coal followed by formation of iron-enriched melt droplets of FeO–SiO₂–Al₂O₃–CaO–MgO composition. Under cooling the melts crystallize with formation of the iron oxide phases, predominantly the ferrite spinel phase (Fe-spinel) which provides the magnetic properties to ferrospheres.²⁴ The yield of ferrospheres from different coal fly ashes ranges from 0.5 to 18.1%, their iron content varies in the range of 20-88 wt. % in terms of Fe₂O₃, and the globule size ranges from 2–3 to hundreds of microns, with a maximum in the particle size distribution at 40 to 150 μm.²³ Ferrosphere fractions of stabilized composition and morphology are available via the multi-step separation of a ferrosphere concentrate by size, density and magnetic characteristics. All fractions of ferrospheres with an iron content of 30-80 wt. % Fe₂O₃ include alumino-magnesium ferrite spinel with phase composition and morphology of the globules being determined by FeO–SiO₂–Al₂O₃ system.²³ The ferrospheres are characterized by a high content of an amorphous aluminosilicate phase (26-62 wt. %) which is inversely proportional to the iron content. At the iron content of more than 80 wt. % Fe₂O₃, CaO-promoted ferrite spinel is formed in ferrospheres. In this case the properties of Fe_xO_y–CaO–SiO₂ system determine the composition and structure of phases. The amount of the amorphous phase is considerably lower (9-24 wt. %) and it is of iron-calcium silicate composition.²³

Aluminosilicate-bearing ferrospheres are of the most interest for the synthesis of core-shell systems with the aluminosilicate amorphous phase being a precursor of the

porous siliceous covering. In the case of synthesis of an additional silica layer, the parent aluminosilicate constituent as a source of surface silanol groups [Si–OH] can provide the strong anchoring silica by means of covalent Si–O–Si binding.

Fabrication of an analogous affine magnetic sorbent derived from ferrospheres with an iron content of about 84 wt. % in terms of Fe₂O₃ has been reported by Frank et al.²⁵ As the starting ferrospheres had a very low content of an aluminosilicate part (no more than 6 wt. %), the silica shell was additionally synthesized by a sol-gel method. In spite of the high specificity with respect to a recombinant protein, the reported sorbent suffers from the fast lost of the sorption capacity due to the weak binding of silica on the surface of ferroferric oxide globules.

To solve the problem of the siliceous shell anchoring, in this paper, we demonstrate alternative ferrosphere-derived magnetic composites for protein separation, such as Ni²⁺-zeolite/ferrosphere and Ni²⁺-silica/ferrosphere beads having the meso- and microporous siliceous coverings with incorporated nickel ions. Starting from aluminosilicate-bearing ferrospheres, two routes were suggested to synthesize porous siliceous shells (Scheme 1), such as (i) hydrothermal treatment of ferrospheres in an alkaline media at 100°C resulting in a microporous zeolite shell (zeolitization route – ZR) and (ii) hydrothermal treatment of ferrospheres – tetraethylorthosilicate (TEOS) – hexadecyltrimethylammonium bromide (CTAB) mixture at 80°C followed by calcination at 500°C with formation of a mesoporous silica shell onto a dense siliceous glass film (template sol-gel route – TR) (Scheme 1, A). The similar synthetic procedures differed by addition of a required quantity of Si- and Al-sources were applied to modify the surface of ferrospheres with a less content of a siliceous amorphous phase (Scheme 1, B).



Scheme 1. Synthetic procedures for fabrication of Ni²⁺-zeolite/ferrosphere beads (ZR-1, ZR-2) and Ni²⁺-silica/ferrosphere (TR-1, TR-2) beads

1. Experimental

1.1 Chemicals and materials

Ferrosphere materials were two narrow 0.063-0.05 mm fractions with different iron contents (Samples Fs-59, Fs-76) produced as provided by separation procedure of magnetic concentrates reported earlier.²³ The magnetic concentrates from fly ashes of two types (Sialic and Ferrisialic) resulted from industrial pulverized combustion of two coals (Ekibastuz basin, Kazakhstan and Tugnuv mine, Russia, accordingly) were the source materials for separation. Figure 1 shows typical views of the initial ferrosphere fractions. Chemical and mineral compositions, values of a bulk density, specific surface area (SSA), specific saturation magnetization (SSM) at 77 K and nickel content of the initial ferrosphere fractions are summarized in Tables 1 and 2.^{23,24}

Reagents for the sodium dodecylsulfate polyacrylamide gel electrophoresis (SDS-PAGE) were acrylamide and bisacrylamide (Medigen, Russia); tetramethylethylenediamine, SDS, and ammonium persulfate (Bio-Rad, USA). The protein standards were from BioRad, USA. The protein markers contained the following proteins (kDa): phosphorylase b (90), bovine serum albumin - BSA (67), ovalbumin (45), carbonic anhydrase (31), soybean trypsin inhibitor (21.5), and lysozyme (14.4). Imidazole, urea, Tris-OH, dithiothreitol (DTT), EDTA (Sigma-Aldrich, USA), and ammonium nitrate were of an analytical grade quality.

All other chemicals used in this work were of a reagent grade quality obtained from commercial suppliers and used without further purification.

1.2 Synthetic procedures

Synthesis of Ni²⁺-zeolite/ferrosphere beads

Ni²⁺-zeolite/ferrosphere beads were prepared by the zeolitization route followed by incorporation of nickel ions onto the zeolite shell (Scheme 1, ZR-1, ZR-2).

Starting from ferrospheres Fs-59 (Scheme 1, ZR-1), the zeolite covering was synthesized without addition of Al- and Si-sources by the hydrothermal treatment of ferrospheres in an alkaline solution at 100°C and autogenous pressure in the ambient atmosphere. In a typical synthesis, a ferrosphere sample (10 g) was mixed with 1.5M aqueous NaOH solution in a 65 ml Teflon autoclave followed by heating the suspension for 24 h under stirring by rotation of the autoclave (30 min⁻¹). The liquid/solid (Fs) ratio by volume was 5:1. Then the product was separated by filtration, washed with distilled water and dried at 80°C. Magnetic microsphere particles were separated from non-magnetic matter by magnetic separation using a hand magnet. The purity of separated magnetic fraction was controlled by means of an optical microscope (Sample Na-Z/Fs-59).

The resulted Na⁺-zeolite/ferrosphere beads were loaded with Ni²⁺ via the ion exchange reaction of Na⁺ for Ni²⁺ by contacting 450 mg/L Ni²⁺ solution in proportion of 0.1:10 (w/v) for 24 hours at a room temperature. The Ni²⁺ loaded solid was filtered off on paper, washed with distilled water and air-dried

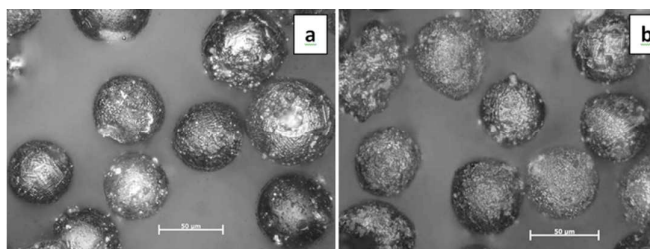


Fig.1 Optical images of initial ferrosphere fractions Fs-59 (a) and Fs-76 (b)

Table 1 Macrocomponent composition, bulk density, specific surface area and nickel content of initial ferrosphere fractions

Sample	Content, wt.%			d, g·cm ⁻³	SSA, m ² ·g ⁻¹	NiO, wt. %
	SiO ₂	Al ₂ O ₃	Fe ₂ O ₃			
Fs-59	26.5	9.4	59.8	1.40	1.3	0.002
Fs-76	9.5	4.6	76.2	1.91	0.4	0.003

Table 2 Phase composition (wt. %) and specific saturation magnetization of initial ferrosphere fractions

Sample	Crystal phases				Glass phase	SSM, emu·g ⁻¹
	ferrosphenel	hematite	quartz	mullite		
Fs-59	48.8	2.9	3.1	3.5	41.2	35.8
Fs-76	67.0	3.8	1.3	-	27.2	57.0

at 100°C for 1 h. The amount of trapped Ni²⁺ was calculated as the solid phase equilibrium Ni²⁺ concentration (Q_e) according to equation (1):

$$Q_e = (C_0 - C_e) \cdot V / m_s \quad (1)$$

where C₀ – Ni²⁺ concentration in initial solution, mg·l⁻¹; C_e – equilibrium Ni²⁺ concentration in an aqueous phase after sorption, mg·l⁻¹; V – aliquot, ml; m_s – mass of solid, mg. The C₀ and C_e values were measured by atomic absorption spectroscopy (Sample Ni,Na-Z/Fs-59).

Starting from ferrospheres Fs-76 (Scheme 1, ZR-2), the zeolite covering was synthesized with addition of Al- and Si-sources. In a synthesis in the presence of Al- and Si-sources, a ferrosphere sample (10 g) was mixed with 1.5M Al(OH)₃ alkaline solution (1.5M NaOH) in a 250 ml polypropylene autoclave followed by addition of liquid sodium glass solution (2M SiO₂) under stirring. The (Al(OH)₃-NaOH)/Fs/SiO₂ solution ratio by volume was 50:1:50. The reaction mixture was hydrothermally treated at 100°C for 72 h under agitation. Thereafter the sediment was filtered and washed out with distilled water. Magnetic particles were separated from the non-magnetic residue in a wet condition using a hand magnet and then dried at 60°C. The purity of separated magnetic fraction was controlled as described above (Sample Na-Z/Fs-76).

The part of zeolitized ferrospheres was converted to NH₄⁺-form by the ion exchange reaction contacting NH₄Cl solution.

To prepare Ni²⁺-zeolite/ferrosphere beads, the NH₄⁺-zeolite/ferrosphere beads were impregnated with 2%

Ni(CH₃COO)₂ solution in proportion of 1:0.8 (w/v), dried at 80°C and calcined at 500°C for 6 h. Magnetic Ni-ferrosphere beads were separated from the unbound NiO fine particles by repeated wet magnetic separation using a hand magnet and then dried at 60°C. The purity of separated magnetic fraction was controlled as described above. The Ni²⁺ loading was controlled by SEM-EDS (Sample Ni-Z/Fs-76).

Synthesis of Ni²⁺-silica/ferrosphere beads

Ni²⁺-silica/ferrosphere beads were prepared by the template sol-gel route followed by incorporation of nickel ions onto the silica shell (Scheme 1, TR-1, TR-2).

The mesoporous silica covering onto the ferrosphere surface was synthesized both in an acid and basic medium using tetraethyl orthosilicate (TEOS) as a silicon source and hexadecyltrimethylammonium bromide (CTAB) as a structure directing template.

In a typical synthesis at a low pH, a ferrosphere sample (2 g) was added to hydrochloric acid solution of CTAB and TEOS with the following composition (mol.): 0.13TEOS:0.11CTAB:0.9HCl:100H₂O. The liquid/solid (Fs) ratio was 20:1 (v/v). The mixture was aged in a 65 ml Teflon autoclave at 80°C for 120 h without agitation. Thereafter the particles were collected by filtration, washed with distilled water, dried at 80-120°C and calcined at 540°C for 4 h. Magnetic particles were separated from non-magnetic phase by magnetic separation (Samples SiO₂/Fs-76-1, SiO₂/Fs-59-2). Another synthesis was carried out under stirring at 80°C for 144 h using the reaction mixture of the following composition (wt. %): 0.06CTAB:0.13TEOS:100H₂O:7HCl. The liquid/solid (Fs) ratio was 25:1 (v/v) (Sample SiO₂/Fs-76-3). The pure SiO₂ was synthesized as described for the sample SiO₂/Fs-76-1 and SiO₂/Fs-59-2 but without adding Fs.

To immobilize Ni²⁺, the silica/ferrosphere beads were activated by boiling in water, impregnated with 2% Ni(CH₃COO)₂ in proportion of 0.3:1 (w/v), dried at 80°C and calcined at 500°C for 4 h. Magnetic Ni-ferrosphere beads were separated from the unbound NiO fine particles as described above. The Ni²⁺ loading was controlled by SEM-EDS (Samples Ni-SiO₂/Fs-59-2, Ni-SiO₂/Fs-76-3).

1.3 Protein separation

To produce recombinant green-fluorescent protein from the bioluminescent jellyfish *Clytia gregaria* (10His-cgreGFP)²⁶ *E. coli* cells XL1-Blue carrying the pQE-cgreGFP25 plasmid were cultivated in Luria-Bertani medium containing 200 µg·ml⁻¹ ampicillin at 37°C until the culture reached an OD₆₀₀ of 1.0. Then for induction of synthesis, 0.5 mM IPTG was added and the cultivation was continued overnight at room temperature for better cgreGFP maturation. Next day the flask containing the liquid culture was refrigerated at 4°C and kept there for two days in order to provide the maximal yield of matured cgreGFP. Cells were harvested by centrifugation, the pellet was resuspended in TBS (20 mM Tris-HCl pH 7.0, 0.15 M NaCl) in proportion of 1:5 (w/v),

disrupted by sonication (20 s x 6) at 0°C and the mixture was centrifuged. The pellet was discarded; supernatant used for experiments on cgreGFP purification with the use of magnetic Ni-ferrosphere beads. The supernatant 500 µl aliquots were mixed with the portion of Ni-ferrosphere beads (40-50 mg) for 20-30 min at room temperature. Then the particles were fixed on the bottom using a magnet and the solution was picked out. The particles were washed with 3 portions of TBS, containing 5 mM imidazole, and then cgreGFP was eluted with 500 µl of 0.5 M imidazole in TBS. The same purification procedure was carried out in the presence of 10 mM EDTA in all solutions.

1.4 Characterization

Chemical composition of ferrosphere fractions was determined according to State Standard (GOST) No. 5382-91.²⁷ Nickel content in initial ferrospheres was determined by the inductively coupled plasma mass spectrometry (ICP-MS) using ELAN-9000 (Perkin-Elmer, USA) instrument.

The phase composition was studied by the X-ray powder diffraction (XRPD) analysis using the Rietveld formalism²⁸ and the derivative difference minimization (DDM) method²⁹ of full-profile refinement. The XRPD data were collected on a PANalytical X'Pert PRO diffractometer equipped with a PIXcel detector and a secondary graphite monochromator for Cu K_α radiation. The quantitative phase analysis with the account for the amorphous component was performed using the external standard method for which the mass absorption coefficients of the samples were derived from their elemental compositions.

To study morphology of the samples JEOL JSM-7001F (Shimadzu, Japan), TM-1000 and TM-3000 (Hitachi, Japan) scanning electron microscopes were used. The optical microscopy observations were performed on an Axio Imager D1M (Carl Zeiss, Germany) optical microscope equipped with a Carl Zeiss AxioCam MRC5 digital color video camera. To study elemental composition the SEM-EDS examination of surfaces and polished sections of ferrospheres and ferrosphere based composites was performed using a TM-3000 microscope equipped with the Bruker microanalysis system including an energy-dispersive X-ray spectrometer with an XFlash 430 H detector and QUANTAX 70 software. The polished sections of ferrospheres were prepared by fixing in an epoxy resin with successive grinding and polishing with use of STRUERS materials and equipment followed by the deposition of a platinum layer of ~20 nm thicknesses. Analysis was carried out at an accelerated voltage of 15 kV in a mapping mode. The data accumulation time was determined by the quality of the spectrum assembly and was found to be at least 10 min.

The porous structure was examined by measuring the nitrogen adsorption-desorption isotherms at 77 K using a Nova3200e (Quantachrome Instruments, USA) and ASAP 2420 V2.02 J (Micromeritics, USA) surface area and pore size analyzers. The specific surface area was calculated by the Brunauer-Emmett-Teller (BET) method under a standard technique.³⁰ The pore size distribution was determined from the isotherm adsorption branch by the classic BJH method.

Infrared spectra were registered on a FT-IR spectrometer Tensor 27 (Bruker, Germany) in the range of 400-4000 cm^{-1} using the standard technique of tableting samples with KBr.

Thermogravimetric (TG) measurements were performed in a Netzsch STA Jupiter 449C device with Aeolos QMS 403C mass-spectrometer under dynamic argon-oxygen (20% O_2) atmosphere, 50 $\text{ml}\cdot\text{min}^{-1}$ total flow rate. Platinum crucibles with perforated lids were used, and the sample mass taken for STA experiments was 20 mg. The measurement procedure consisted of a temperature stabilization segment (30 min at 40°C) and a dynamic segment at heating rate of 10 $^\circ\text{C}\cdot\text{min}^{-1}$. Qualitative composition of the evolved gases was determined by on-line QMS in Multiple Ion Detection mode. The following predefined ions were scanned: $m/z = 18$ (H_2O), 28 (N_2 , CO), 30(NO), 32 (O_2), 40(Ar), 44(CO_2).

The adsorption capacity of the sorbents regarding 10His-cgreGFP was evaluated according to the difference of solution optical densities (OD) at the 485 nm wave length before and after protein adsorption using the 10His-cgreGFP molar extinction coefficient (E) in the green part of the spectrum ($E_{485} = 63030 \text{ M}^{-1}\cdot\text{cm}^{-1}$).²⁶ TBS was used as a reference solution. Desorption value was determined from the OD_{485} of 10His-cgreGFP solution resulted from eluting NFBs by 0.5 M and 1.5 M imidazole in TBS. 0.5 M or 1.5 M imidazole in TBS was used as a reference solution. UV absorbance spectra were registered using a SmartSpecPlus spectrophotometer (BioRad, USA).

The affinity of 10His-cgreGFP separation from the cell lysate was detected by the 12.5% SDS-PAGE.

2. Results and discussion

Zeolitization route

Based on the experience in fabrication of microsphere zeolite materials by zeolitization of coal fly ash cenospheres composed of aluminosilicate glass with $\text{SiO}_2/\text{Al}_2\text{O}_3 = 2.2-3.2$ (w/w),^{31,32} a NaP zeolite phase with a gismondine topology (GIS) was expected to crystallize under the similar hydrothermal treatment of an aluminosilicate precursor with $\text{SiO}_2/\text{Al}_2\text{O}_3 = 2.8$ being part of the ferrospheres Fs-59. As it has been reported,^{31,32} a zeolite layer on the surface of aluminosilicate microspheres is generated through dissolution step of aluminosilicate glass under stirring in an alkaline solution favoring the equalization of silicate and alkaline concentrations both in the solution and the microsphere layer. Oligomeric silicate and aluminosilicate building units formed in the reaction medium undergo further polymerization on the nuclei enriched solid surface of the undissolved matter resulting in a zeolite framework.

The 6.1 and 3.6 wt. % NaP phase was identified in modified ferrospheres Fs-59 and Fs-76, respectively, by the XRPD method (Fig. 2, Table 3), the NaP phase being the single zeolitic phase in both products.

Figure 3 gives SEM images of the ferrosphere surfaces after the hydrothermal treatment without and with adding Si- and Al-sources (Fig. 3 a, b and Fig. 3 c, d, respectively). The continuous layer of columnar-shaped crystallites oriented normally to the surface of not transformed matter is revealed

in the products (Fig. 3 b, d). The NaP zeolite is a crystalline aluminosilicate with pore sizes of 3.1 x 4.4 and 2.8 x 4.9 Å providing a microporosity of the coating shell.³³ As it was established by the N_2 adsorption-desorption method for Na-Z/Fs-59, the pore size distribution (PSD) in the range of 10-900 Å has a maximum at about 25 Å pointing to the presence of mesopores in the zeolitic covering. Due to the microporosity the specific surface area of the zeolitized beads was about 21 $\text{m}^2\cdot\text{g}^{-1}$ (Table 3).

The main difference of the Na-Z/Fs-76 from Na-Z/Fs-59 is the lower SSA value (6.4 $\text{m}^2\cdot\text{g}^{-1}$). The PSD for the given sample is polymodal without well-defined maxima reflecting the intercrystallite porosity.

The water content in zeolitized samples is shown in Figure 4 (wt.%). According to TG data, a progressive mass loss was observed at 40-380°C for all samples studied. This mass loss is obviously ascribed to water desorption according to the mass-spectral analysis of the gases evolved. The zeolitized samples are differed by water content values correlating with the content of the NaP phase in the samples (Table 3).

Figure 5 shows Al, Si and Fe distributions over a cross-section of Fs-59 ferrosphere globule before and after zeolitization. It is obviously that Si and Al being located primarily in an intercrystalline space of the untreated ferrosphere globule concentrated in the surface region of the modified globule forming an aluminosilicate shell over the magnetic core.

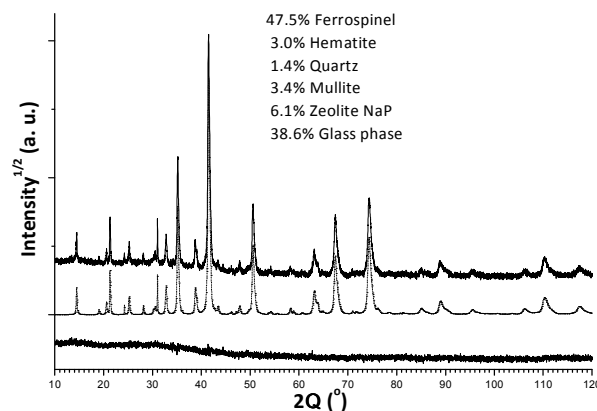


Fig. 2 Observed (top line), calculated (dashed line) and difference (bottom line) XRPD patterns of sample Na-Z/Fs-59

Table 3 Texture characteristics of zeolitized ferrospheres

Sample	Zeolite phase	Content, wt. %	D_{max} , Å	V_{meso} , $\text{cm}^3\cdot\text{g}^{-1}$	SSA, $\text{m}^2\cdot\text{g}^{-1}$
Na-Z/Fs-59	NaP	6.1	25	0.036	21
Na-Z/Fs-76	NaP	3.6	not available	0.020	6.4

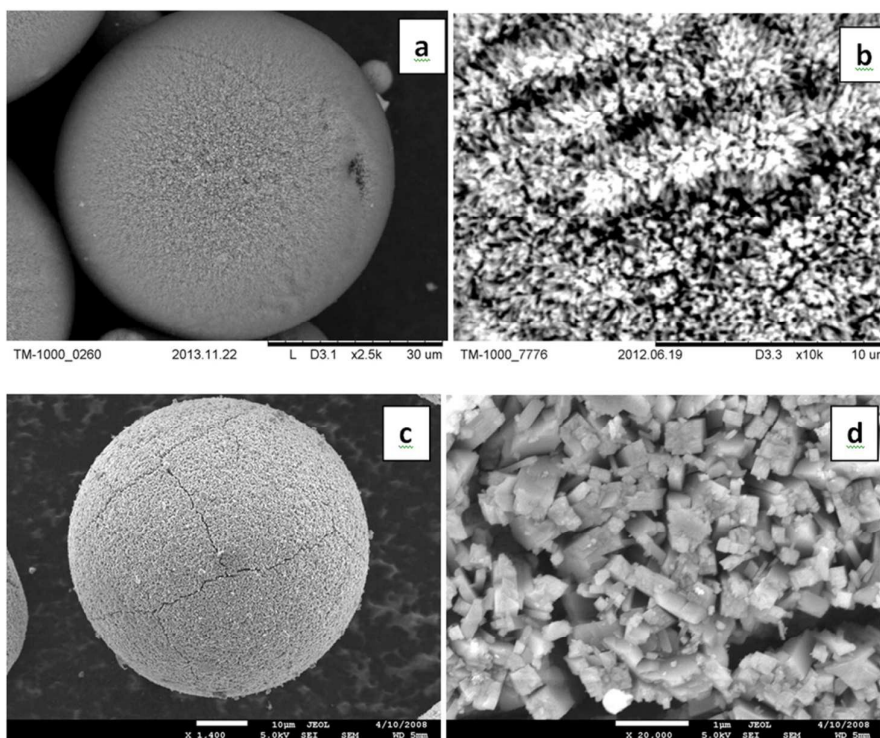


Fig. 3 SEM images of zeolitized ferrospheres Na-Z/Fs-59 (a, b) and Na-Z/Fs-76 (c, d)

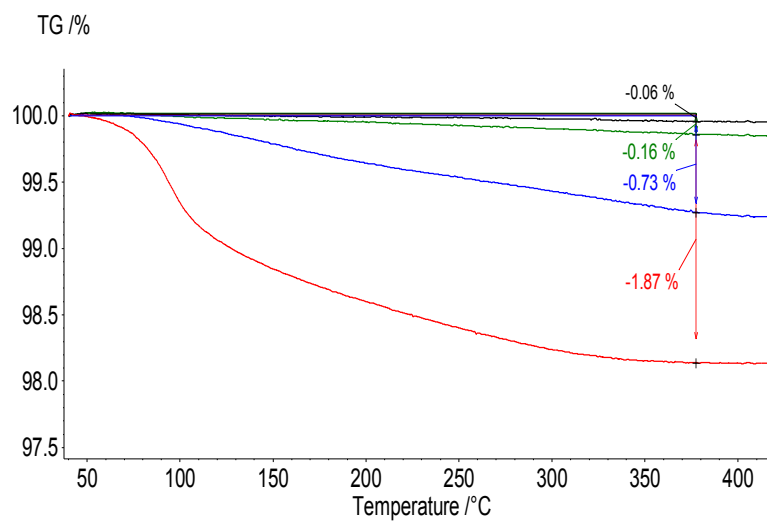


Fig. 4 TG curves for thermal transformation of Na-Z/Fs-59 (red), Na-Z/Fs-76 (blue), SiO₂/Fs-76-3 (green) and SiO₂/Fs-59-2 (black).

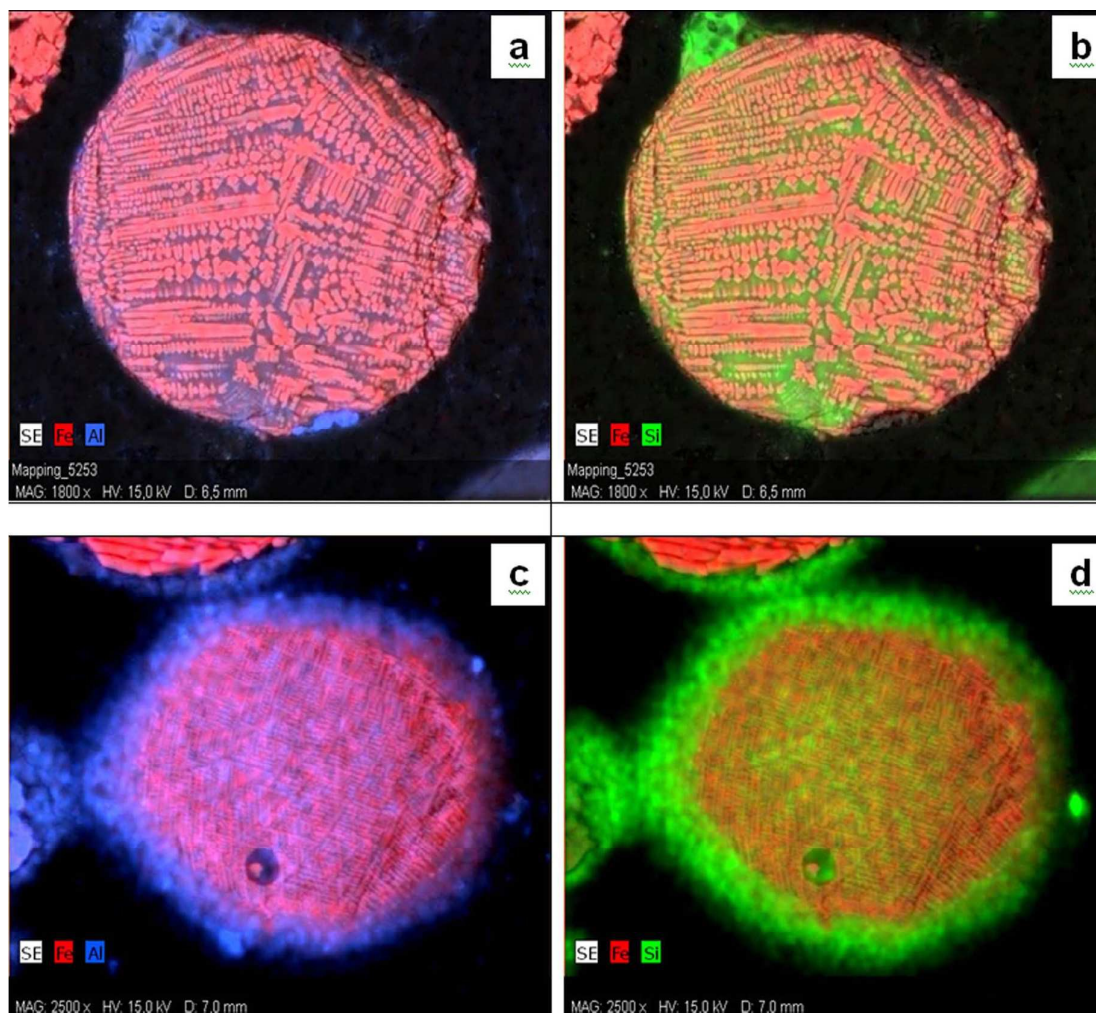


Fig. 5 Distribution of Al, Si and Fe over a cross-section of a Fs-59 ferrosphere globule: initial (a, b) and with the zeolitic covering (c, d)

Due to the ion exchange ability of zeolites, incorporation of nickel ions into the zeolite layer of sample Fs-59/Na-Z has been realized according to reaction $\text{NaP} + 0.5\text{Ni}^{2+} \leftrightarrow 0.5\text{NiP} + \text{Na}^+$. The resultant Ni^{2+} loading of the sample was $0.12 \text{ mmol}\cdot\text{g}^{-1}$. Another method applied to sample Na-Z/Fs-76 targeted formation of NiO clusters in the zeolite pores.³⁴ The Ni^{2+} loading for this sample was $0.09 \text{ mmol}\cdot\text{g}^{-1}$. The Ni^{2+} distribution over the surface of a Ni-Z/Fs-76 globule by the SEM-EDS data is shown in Figure 8.

Template sol-gel route

Figure 6 displays SEM images of silica/ferrosphere beads obtained in an acid reaction medium. As it follows from the data, the composite beads $\text{SiO}_2/\text{Fs-76-3}$ prepared in dynamic conditions are covered by the continuous silica film (Fig. 6 a). Based on the detailed study of cracks in the shell, its thickness was evaluated to be 0.2-0.3 microns. On the contrary, sample $\text{SiO}_2/\text{Fs-76-1}$ synthesized in static conditions is characterized by the fragmentary coating. The covering of sample Fs-59 is also

Table 4 Texture characteristics of ferrospheres with the silica covering

Sample	SiO ₂ content, wt. %	D _{max} , Å	V _{meso} , cm ³ ·g ⁻¹	SSA, m ² ·g ⁻¹
SiO ₂	100	22	0.592	1154
SiO ₂ /Fs-76-1	4	26;45	0.022	21
SiO ₂ /Fs-59-2	~1	27	0.010	11
SiO ₂ /Fs-76-3	6	n.d.*	n.d.	24

* not determined

partial making visible the texture of the ferrosphere surface (Fig. 6 b). The SSA value (11 m²·g⁻¹) of the sample SiO₂/Fs-59-2 corresponds to the silica content of about 1 wt. %. The difference in elemental composition of two surface sites,

covered and uncovered by the silica film, is presented in Figure 6.

Table 4 shows textural parameters of the individual SiO₂ and samples prepared by the similar method. As for pure SiO₂, its N₂ adsorption-desorption isotherm is typical for microporous materials with the monomodal PSD having the pore width maximum at 22 Å and SSA of about 1000 m²·g⁻¹. This pore size value belongs to the boundary region between micro- and mesostructured porous materials.³⁴ The small pore size compared to the similar one of classic silicate mesoporous materials synthesized in a basic medium (for example, MCM-41 with D=41 Å³⁵) can be explained by the low pH value of the reaction mixture.³⁶ The porosity of composite silica-bearing globules is also characterized by prevailing pores with widths of lower than 30 Å (Table 4). In the case of sample SiO₂/Fs-76-1, two maxima at 26 and 45 Å are being defined at the pore size distribution curve pointing to the biporous structure.

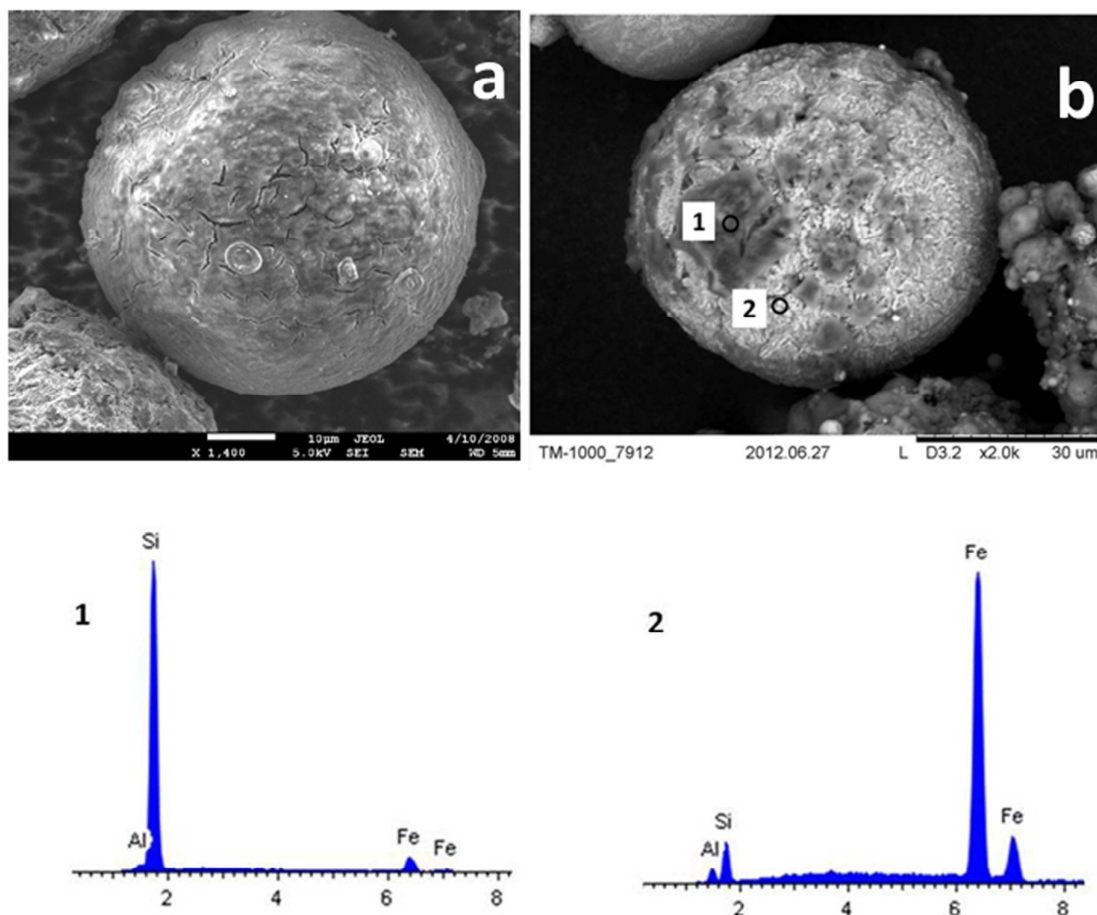


Fig.6 SEM images of ferrosphere globules with the SiO₂ covering for samples (a) SiO₂/Fs-76-3 and (b) SiO₂/Fs-59-2, and distribution of Si and Fe for sample SiO₂/Fs-59-2 (spots 1, 2)

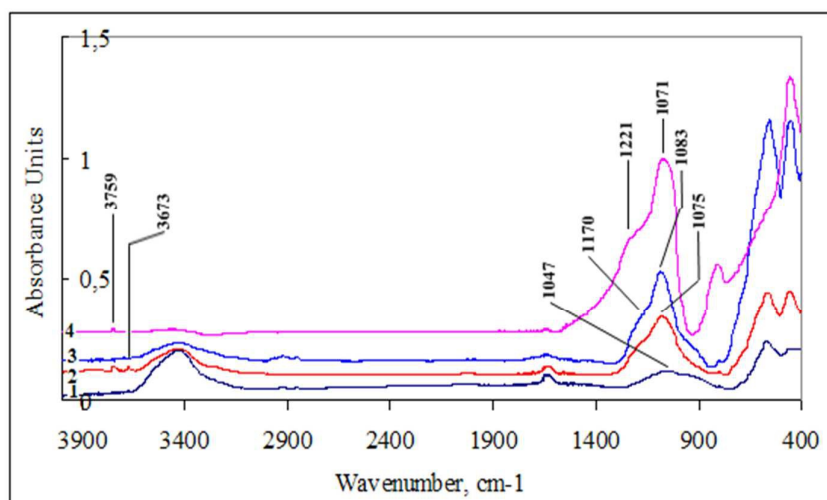


Fig. 7 IR spectra of SiO_2 , initial ferrosphere fraction Fs-76 and silica/ferrosphere beads: 1 - Fs-76; 2 - $\text{SiO}_2/\text{Fs-76-1}$; 3 - $\text{SiO}_2/\text{Fs-76-3}$; 4 - SiO_2

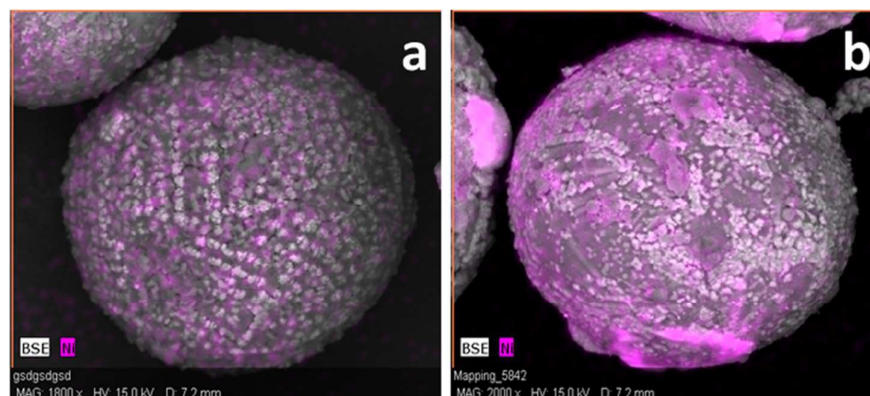


Fig. 8 Distribution of Ni over a surface of ferrosphere globules with the zeolite and SiO_2 covering for samples (a) Ni-Z/Fs-76 and (b) Ni- $\text{SiO}_2/\text{Fs-59-2}$.

IR absorption spectra of pure silica and silica/ferrosphere beads based on sample Fs-76 are presented in Figure 7. From comparison of the sample Fs-76 spectrum (curve 1 in Figs. 7) with spectra of ferrosphere supported silica (curves 2, 3 in Fig. 7) one can distinctly see changes in the spectral patterns. In the absorption spectra the increase of intensities of absorption bands in the field of Si-O valent ($1200\text{-}1000\text{ cm}^{-1}$) and deformation ($750\text{-}400\text{ cm}^{-1}$) vibrations is observed. A new 560 cm^{-1} absorption band which is characteristic for pure silica appears. The similar changes are also observed in the diffusion reflection spectra. In general, these facts evidence about the occurrence of silica in the ferrosphere based composites. Shifts of absorption bands of Si-O valent vibration to a high frequency field (58 and 66 cm^{-1} for $\text{SiO}_2/\text{Fs-76-3}$ and $\text{SiO}_2/\text{Fs-76-1}$, respectively) point to the chemical binding of silica with reactive sites of the ferrosphere surface. As for free silanol OH-groups, in the absorption and diffusion reflection spectra these are distinctly seen as a doublet of absorption bands at 3750 и 3673 cm^{-1} only for sample

$\text{SiO}_2/\text{Fs-76-1}$ prepared without agitation. The SiO_2 loading values calculated from the difference of optical densities and integral intensities in the field of valent vibrations of Si-O groups were 6 and 4 wt. % for $\text{SiO}_2/\text{Fs-76-3}$ and $\text{SiO}_2/\text{Fs-76-1}$, respectively (Table 4).

As it follows from the TG data (Fig. 4), the water content in the sol-gel samples are considerably lower than in the zeolitized samples. The water losses also correlate with the SiO_2 content in the samples (Table 4).

For further modification of silica/ferrosphere beads by immobilizing nickel ions in a silica shell, samples $\text{SiO}_2/\text{Fs-59-2}$ and $\text{SiO}_2/\text{Fs-76-3}$ were used. The first one is an analogue of $\text{SiO}_2/\text{Fs-76-1}$ which has the more reactive surface. The latter silica/ferrosphere beads were selected by reason of the high silica content (6 wt. %). To load Ni^{2+} ions impregnation with Ni^{2+} salt solution followed by calcination has been undertaken. The sample $\text{SiO}_2/\text{Fs-59-2}$ was preliminary activated by boiling in water resulting in an increase of surface hydroxyl group concentration due to the hydrolysis of siloxane bonds.³⁷ It was supposed that thermal

decomposition of the Ni^{2+} salt at the calcination step would give covalently bound Ni^{2+} forms, such as NiO particles located in pores and/or nickel silicates via interaction of Ni^{2+} with oxygen atoms of the surface silanol groups.³⁸ The starting Ni^{2+} loading on every sample was about $0.3 \text{ mmol}\cdot\text{g}^{-1}$. The Ni^{2+} presence on the surface of a $\text{Ni-SiO}_2/\text{Fs-59-2}$ globule is evidenced by the SEM-EDS data (Fig. 8b).

Protein affinity separation

To evaluate the particles affinity the recombinant green fluorescent protein from medusa *Clytia gregaria* (cgGFP) containing 10-His tag on the N-end was used (10His-cgGFP). This protein is a convenient model for our investigations due to its unique spectral properties – fluorescence under UV-irradiation ($\lambda_{\text{max}} = 500 \text{ nm}$) and absorption spectrum displaying two peaks at 278 nm and 485 nm with molar extinction coefficients of 38650 and $63030 \text{ M}^{-1}\cdot\text{cm}^{-1}$, respectively²⁶. So the protein purification can be monitored visually according to the solutions green fluorescence or spectrophotometrically according to its absorbance at 485 nm. Table 5 displays the calculated values of the NFB binding capacity with respect to protein at the adsorption step and eluted amount of the protein from NFB after adsorption at different concentrations of imidazole in an eluting solution.

As it follows from data presented, the amount of trapped protein varied in the range of $0.8\text{-}3.0 \text{ mg}\cdot\text{g}^{-1}$, or $1.5\text{-}5.7 \text{ mg}\cdot\text{cm}^{-3}$ depending on preparation of NFB samples and initial protein concentration. About 50-70 % of the protein is washed off in 0.5M imidazole, and the amount of eluted protein increased with increasing imidazole concentration up to 1.5 M. The same effect was also observed by *Wu et al.*⁹ By the example of sample Ni-Z/Fs-76 it was established that NFB capacities increased about two times more as the initial protein concentration increased (Table 5). Samples Ni-Z/Fs-76 and Ni-SiO₂/Fs-59-2 demonstrated best adsorption capacities and reusability up to six times.

Table 5 Adsorption capacity of Ni^{2+} -zeolite/ferrosphere and Ni^{2+} -silica/ferrosphere beads in protein affinity separation

Sample	Adsorbed amount, ^a		Eluted amount	
	$\text{mg}\cdot\text{g}^{-1}$	$\text{mg}\cdot\text{cm}^{-3}$	in 0.5 M imidazole, $\text{mg}\cdot\text{g}^{-1}$	in 1.5 M imidazole ^f , $\text{mg}\cdot\text{g}^{-1}$
Ni ₂ Na-Z/Fs-59	1.5	2.1	0.4	n.d.
Ni-Z/Fs-76	1.7	3.2	1.0	0.6
	2.2 ^b	4.2	1.1	0.5
	3.0 ^c	5.7	2.0	0.2
Ni-SiO ₂ /Fs-59-2	1.3 ^d	1.8	0.5	n.d.
	1.1	1.5 ^e	0.5	n.d.
	1.0	1.4	0.5	0.6
Ni-SiO ₂ /Fs-76-3	0.8	1.5	0.3	0.4

^a determined at initial optical density $\text{OD}_{485} = 0.454$; ^b $\text{OD}_{485} = 0.69$; ^c $\text{OD}_{485} = 1.27$; ^d 1-4 runs; ^e separation in the presence of 10 mM EDTA; ^f additionally eluted

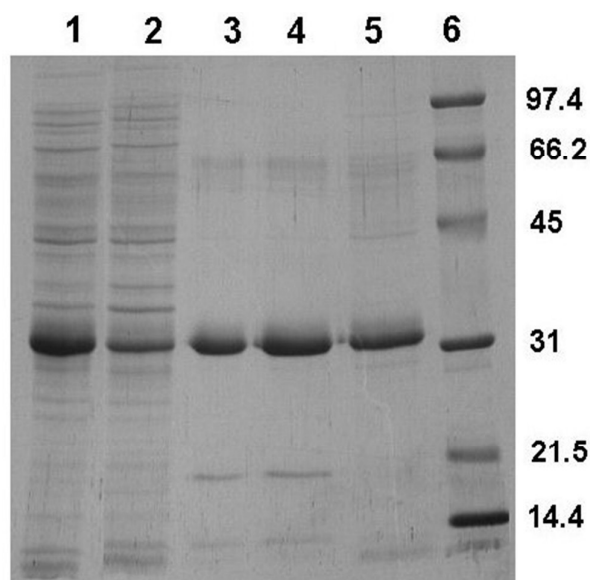


Fig. 9 12.5% SDS-PAGE analysis of 10His-cgGFP purification on Ni-Z/Fs-76 (2–4 lanes) and Ni-SiO₂/Fs-59-2 (5 lane) beads. Lanes: 1 – initial mixture (recombinant *E. coli* cells cytoplasm); 2 – outlet flow throw fraction; 3 – 0.5 M imidazole fraction; 4 – 0.5 M imidazole fraction, purification in the presence of 10 mM EDTA; 5 – 0.5 M imidazole fraction (6th run); 6 – standard proteins (BioRad, USA), molecular weights are shown with numbers

Figure 9 shows SDS-PAGE analysis of the recombinant *E. coli* cells cytoplasm and 10His-cgGFP purity at the final step of purification. One-step separation using beads Ni-Z/Fs-76 and Ni-SiO₂/Fs-59-2 yielded a protein purity of up to 95 %. No differences in the protein purity were observed when purification was carried out in the presence of 10 mM EDTA as a chelating agent.

Conclusions

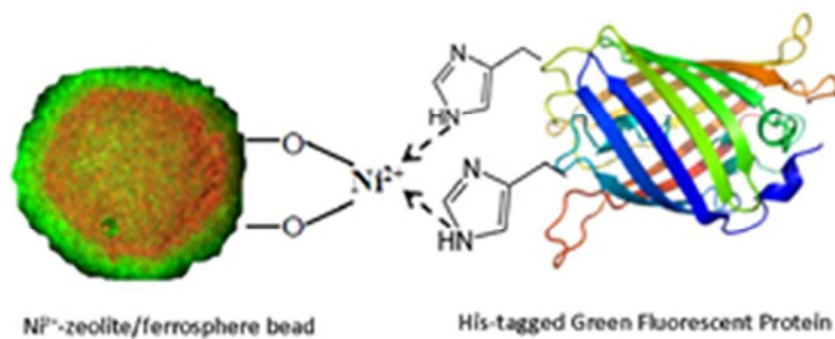
In this paper, we have demonstrated methods for fabrication of ferrosphere-based magnetic beads of a core-shell structure with immobilized Ni^{2+} ions in zeolite and silica shells for affinity separation of recombinant proteins (20-30 kDa). The Ni^{2+} -zeolite/ferrosphere and Ni^{2+} -silica/ferrosphere beads display a strong affinity for His-tagged cgGFP with capacities of $1.5\text{-}5.7 \text{ mg}\cdot\text{cm}^{-3}$. Their selectivity for the His-tagged proteins and recyclability are maintained after recycling 6 times. Ferrospheres as a by-product is an available low-cost magnetic material providing reduction in price for ferrosphere-based functional materials and relatively fast fabrication of enlarged quantities of affine sorbents. We anticipate a continued dissemination of the ferrosphere-based sorbents in the field of purification of recombinant proteins, for example, regarding production of biopharmaceuticals.

Acknowledgements

The work was supported by the State budget allocated to the fundamental research in the Russian Academy of Sciences in the framework of projects No. V. 45.3.1 (preparation and characterization of magnetic affinity sorbents) and No. VI. 57.1.1 (10His-cgrecLGF preparation, protein affinity separation and analyses). The authors acknowledge Dr. E. M. Mazurova for SEM observations, V. V. Yumashev and Dr. V. A. Parfenov for examination of materials porosity, Dr. N. I. Pavlenko and L. A. Solovyev for IR spectroscopy and XRPD studies, respectively, Dr. S. N. Vereshchagin for performance of the thermogravimetric analysis.

References

- C. L. Young, Z. T. Britton and A. S. Robinson, *Biotechnol. J.*, 2012, **7**, 620.
- J. J. Lichty, J. L. Maleck, H. D. Agnew, D. J. Michelson-Horowitz and S. Tan, *Protein Express. Purif.*, 2005, **41**, 98.
- M. Saraswat, L. Musante, A. Ravidá, B. Shortt, B. Byrne, and H. Hothofer, *BioMed Research International*, 2013, **2013**, Article ID 312709, <http://dx.doi.org/10.1155/2013/312709>
- V. Gabert-Porecar and V. Menart, *J. Biochem. Biophys. Methods*, 2001, **49**, 335.
- H. Block, B. Maertens, A. Spriestersbach, N. Brinker, J. Kubicek, R. Fabis, J. Labahn, F. Schafer, *Methods in Enzymology*, 2009, **463**, 439.
- S. Knecht, D. Ricklin, A. N. Eberle and B. Ernst, *J. Mol. Recognit.*, 2009, **22**, 270.
- R. K. Scopes. *Protein purification: principles and practice*. – 3rd Ed., Springer-Verlag, 1994, 380 p.
- D. J. Wang, D. J. Zhang, F. Xu, W. Shan, G. B. Zhu, P. Y. Yang and Y. J. Tang, *Stud. Surf. Sci. Catal.* 2004, **154**, 2027.
- Y. Wu, G. Chang, Y. Zhao and Y. Zhang, *Dalton Trans.*, 2014, **43**, 779.
- A. Frenzel, C. Bergemann, G. Kohl and T. Reinard, *J. Chromatogr. B*, 2003, **793**, 325.
- M. Bele, G. Hribar, S. Campelj, D. Makovec, V. Gaberc-Porekar, M. Zorko, M. Gaberscek, J. Jamnik and P. Venturini, *J. Chromatogr. B*, 2008, **867**, 160.
- Y. Wang, G. Wang, Y. Xiao, Y. Yang and R. Tang, *ACS Appl. Mater. Interfaces*, 2014, **6** (21), 19092.
- J. Y. Kim, N. Piao, Y. Lee II, I.-H. Park Lee, J.-H. Lee, S. R. Paik and T. Hyeon, *Adv. Mater.*, 2010, **22**, 57.
- Y. Zhang, Y. Yang, W. Ma, W. Guo, Y. Lin and C. Wang, *ACS Appl. Mater. Interfaces*, 2013, **5** (7), 2626.
- C. L. Chiang, C. Y. Chen and L. W. Chang, *J. Chromatogr. B*, 2008, **864**, 116.
- X. Zou, K. Li, Y. Zhao, Y. Zhang, B. Li and C. Song, *J. Mater. Chem. B*, 2013, **1**, 5108.
- QIAGEN. Ni-NTA Magnetic Agarose Bead Handbook, Hilden, Germany, 12/2001.
- TALON® Magnetic Beads, Clontech Laboratories, Inc., 2006, www.clontech.com.
- Purification of 6xHis-tagged proteins with magnetic SiMAG-IDA/Nickel particles, Protocol B5, Chemicell GmbH, <http://www.chemicell.com>.
- BcMag™ His-Ni Magnetic Beads, <http://www.bioclone.us>.
- Sharonova, O.M.; Anshits, N.N.; Anshits, A.G. *Inorg. Mater.* **2013**, *49*, 586–593.
- Y. Zhao, J. Zhang, J. Sun, X. Bai and C. Zheng, *Energy Fuels*, 2006, **20** (4), 1490.
- O. M. Sharonova, N. N. Anshits, L. A. Solovyov, A. N. Salanov and A. G. Anshits, *Fuel*, 2013, **111**, 332.
- O. A. Bayukov, N. N. Anshits, M. I. Petrov, A. D. Balaev and A. G. Anshits, *Mater. Chem. Phys.*, 2009, **114**, 495.
- L. A. Frank, V. V. Borisova, T. A. Vereshchagina, E. V. Fomenko, A.G. Anshits and I.I. Gitelson, *Appl. Biochem. Microbiol.*, 2009, **45**, 215.
- S. V. Markova, L. P. Burakova, L. A. Frank, S. Golz, K. A. Korostileva and E. S. Vysotski, *Photochem. Photobiol. Sci.*, 2010, **9**, 757.
- Cements and materials for cement production. Chemical analysis methods*, State Standard (GOST) No.5382-91. IPK Izdatel'stvo standartov, Moscow, 2002.
- H. Reitveld, *J. Appl. Cryst.*, 1969, **2**, 65.
- L. A. Solovyov, *J. Appl. Cryst.*, 2004, **37**, 743.
- S. Brunauer, P.H. Emmett and E. Teller, *J. Am. Chem. Soc.*, 1938, **60**, 309.
- T. A. Vereshchagina, S. N. Vereshchagin, N. N. Shishkina, L. A. Solovyov, O. A. Mikhaylova and A. G. Anshits, *Micropor. Mesopor. Mater.*, 2013, **169**, 207.
- T. A. Vereshchagina, S. N. Vereshchagin, N. N. Shishkina, L. A. Solovyov, N. G. Vasilieva and A. G. Anshits, *J. Nucl. Mater.*, 2013, **437**, 11.
- D. Breck. *Zeolite Molecular Sieves: Structure, Chemistry and Use*, Wiley-Interscience Publication, John Wiley&Sons, New York, London, Sydney, Toronto, 1974, 771 p.
- S. J. Gregg and K. S. W. Sing. *Adsorption, Surface Area, & Porosity*, Second Edition, Academic Press, London, 1982, 303 p.
- C. T. Kresge, M. E. Leonwicz, W. J. Roth, G. C. Vartuli and J. S. Beck, *Nature*, 1992, **359**, 710.
- L. Pasqua, F. Testa, R. Aiello, F. Renzo and F.Fajula, *Micropor. Mesopor. Mater.*, 2001, **44-45**, 111.
- M. Cypryk and Y. Apeloig, *Organometallics*, 2002, **21**, 2165.
- M. E. Mahmoud, *Metal Ions: Silica Gel Surface Modification for Selective Extraction*, Encyclopedia of Chromatography, Third edition, 2009. DOI: 10.1081/E-ECHR3-120042798.



Ferrosphere-based magnetic beads of a core-shell structure with immobilized Ni^{2+} having a high affinity towards His-tagged recombinant proteins were fabricated.

39x19mm (300 x 300 DPI)